Valence-Shell Spectra. Valence-shell electron energy loss spectra of $Cr(CO)_6$, $Mo(CO)_6$, and $W(CO)_6$ at a resolution of 0.068 eV fwhm and 3000 eV impact energy are shown in Figure 5 in the energy loss range 4-28 eV together with the corresponding spectrum of free CO. The valence-shell spectra of the metal carbonyls provide an important check of sample purity and in particular clearly confirm the absence of any free CO in the interaction region due to decomposition. In this fashion it has been established that the features in the C 1s and O 1s inner-shell spectra (Figures 2 and 3) are due entirely to the metal carbonyl complexes and not free CO.

The valence-shell electronic spectra of the group VIA metal hexacarbonyls below ~14 eV have been investigated earlier by photoabsorption[12-15] and also by electron energy loss methods at low impact energies.[16] These spectra[12-16] exhibit essentially the same features as those observed in the present work. There are some differences in relative intensities between the present and previous[16] EELS spectra, which can be ascribed to the large differences in the respective impact energies. The energies, term values, and suggested assignments for the numbered features in the spectra shown in Figure 5 are presented in Table V. The assignments for the peaks below the first ionization energies follow those given by Beach and Gray[13] and Koerting et al.[16]

The valence-shell energy loss features above the first ionization energies of the hexacarbonyls cannot be assigned in detail as was also the case for $Ni(CO)_4$.[20] However, we make the following tentative assignments on the basis of the photoelectron spectra of the hexacarbonyls[1,2] and calculated molecular orbital energy levels:[21,24,27-32] (1) The peaks between the $t_{2g}(nd)$ and $(5\sigma + 1\pi)$ edges are assigned to intraligand transitions from the $(5\sigma + 1\pi)$ orbitals to the π^* orbitals. It is possible that the lowest energy transitions in each case correspond to $t_{1u}(5\sigma) \rightarrow \pi^*$. (2) The very broad, low intensity features above the $(5\sigma + 1\pi)$ edges (features 12 and 13 for $Cr(CO)_6$, 12 for $Mo(CO)_6$, and 9 for $W(CO)_6$) are assigned to shape resonances. More detailed assignments of both the valence and inner-shell spectra will only be possible with the guidance of sufficiently accurate theoretical calculations.

Conclusions

We have obtained the C 1s and O 1s ISEELS spectra of $Cr(CO)_6$, $Mo(CO)_6$, and $W(CO)_6$ at high resolution (0.068 eV). The spectra were interpreted by analogy with the corresponding spectra of free CO and our previously reported results for $Ni(CO)_4$. As in the case of $Ni(CO)_4$ (and free CO), intense resonantly enhanced $1s \rightarrow \pi^*$ and $1s \rightarrow \sigma^*$ bands were observed. Vibrational structure associated with a C-O stretching mode was resolved in the C 1s $\rightarrow \pi^*$ bands. This vibrational structure reflects aspects of the metal-ligand bonding in these complexes, in particular the metal $\rightarrow$ CO π^* back-donation. The present work therefore strongly supports the preliminary conclusion in our recent paper on $Ni(CO)_4$ that reasonable assessments of the metal ligand bonding situation in a variety of transition-metal species can be provided by high-resolution inner-shell electron energy loss spectroscopy. Further work in this laboratory is planned to investigate the applicability of the ISEELS method to studies of transitions-metal nitrosyl and mixed nitrosyl/carbonyl complexes.

Acknowledgment. This work has been financially supported by NSERC (Canada). In addition a SERC(UK)/NATO Postdoctoral Fellowship (G.C.) and a University of British Columbia Graduate Fellowship (K.H.S.) are gratefully acknowledged.

Transition Structures of the Lewis Acid Catalyzed Diels-Alder Reaction of Butadiene with Acrolein. The Origins of Selectivity

David M. Birney and K. N. Houk*

Contribution from the Department of Chemistry and Biochemistry, University of California, Los Angeles, Los Angeles, California 90024-1569. *Received February 7, 1989*

Abstract: Four transition structures for the Diels-Alder reaction of butadiene and acrolein complexed with BH_3 have been located with ab initio calculations at the RHF/3-21G level, and activation energies have been calculated with the 6-31G* basis set. These calculations reproduce both the decreased activation energy and the enhanced endo selectivity experimentally observed upon catalysis. The transition structures show significant zwitterionic character, which is related to the greater calculated asynchronicity in the catalyzed reaction as compared to the uncatalyzed one.

The extraordinary influence of Lewis acid catalysts on the rates and both regiochemical and stereochemical selectivities of Diels-Alder reactions[1] has been much exploited in synthesis.[2] Recent studies on the reactions of optically active dienes,[2] dienophiles,[2] and catalysts[3] highlight its importance. The profound effects of catalysis have sparked an extensive series of mechanistic[4] and qualitative theoretical[5] investigations. Such a reaction has not previously been investigated with ab initio theory. We have used RHF/3-21G and 6-31G* calculations to locate the transition structures of a simple process of this type, the cycloaddition of butadiene to acrolein coordinated with BH_3 (eq 1). These calculations provide new insight into the effects of Lewis acid catalysis on the geometry, flexibility, and energy of a Diels-Alder transition structure and the influence of these factors on selectivity.

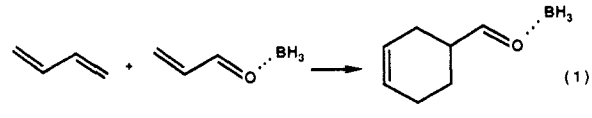

(1)

(1) Inukai, T.; Kojima, T. *J. Org. Chem.* **1971**, *36*, 924-928 and references therein.

(2) (a) Oppolzer, W. *Angew. Chem., Int. Ed. Engl.* **1984**, *23*, 876-889. (b) Paquette, L. A. In *Asymmetric Synthesis*; Morrison, J. D., Ed.; Academic: New York, 1974; Vol. 3. Chapter 4. (c) Masamune S.; Choy, W.; Petersen, J. S.; Sita, L. R. *Angew. Chem., Int. Ed. Engl.* **1985**, *24*, 1-76.

(3) (a) Bednarski, M.; Danishefsky, S. *J. Am. Chem. Soc.* **1986**, *108*, 7060-7067. (b) Kunz, H.; Muller, B.; Schanzenbach, D. *Angew. Chem., Int. Ed. Engl.* **1987**, *26*, 267-269. (c) Chapuis, C.; Jurczak, J. *Helv. Chim. Acta* **1987**, *70*, 436-440.

(4) Sauer, J.; Sustmann, R. *Angew. Chem., Int. Ed. Engl.* **1980**, *19*, 779-807.

(5) (a) Woodward, R. B.; Hoffmann, R. *The Conservation of Orbital Symmetry*; Verlag Chemie: Weinheim, 1970. (b) Houk, K. N.; Strozier, R. W. *J. Am. Chem. Soc.* **1973**, *95*, 4094-4096. (c) Herndon, W. C. *Chem. Rev.* **1972**, *72*, 157-179. (d) Branchadell, V.; Oliva, A.; Bertran, J. *J. Mol. Struct. (Theochem)* **1986**, *138*, 117-120.

0002-7863/90/1512-4127$02.50/0

Table I. Characteristics of the Transition Structures[a] for the Reaction of Butadiene and Acrolein with and without BH_3 Complexation

	catalyzed[b]					uncatalyzed[c]	
	NC[d]	NCA[e]	XC	NT	XT	NCU	NTU
E_{rel}(3-21G), kcal/mol	0.0	0.05	2.2	4.7	7.3	0.0 (12.4)[f]	2.1
E_{rel}(6-31G*), kcal/mol	0.2	0.0	1.5	1.9	4.2	0.0 (7.0)[f]	0.6
C_1–C_6, Å	2.960	2.728	2.588	2.457	2.408	2.353	2.288
C_4–C_5, Å	1.932	1.939	1.971	2.036	2.068	2.088	2.133
C_2–C_7, Å	2.902	2.873	3.686	3.074	3.751	2.945	3.102
C_4–C_5–C_6–C_1, deg	4.48	1.82	−12.27	−17.45	−1.71	2.76	−7.265
charge donation[g]	0.31	0.29	0.26	0.22	0.20	0.09	0.09
coulomb energy[h]	0.0	0.9	8.2	10.1	14.8		
dipole moment, D	8.4	8.6	9.4	10.0	9.6	3.2	4.0

[a] For all structures except NC and NCA, frequency calculations were performed; only one imaginary frequency was obtained in each case. [b] On the basis of the RHF/3-21G optimized geometries. Absolute energies are as follows (hartrees): RHF/3-21G, NC −369.983 95, NCA −369.983 87, NT −369.976 46, XC −369.980 41, XT −369.972 38; RHF/6-31G*, NC −372.030 947, NCA −372.031 200, XC −372.028 479, NT −372.027 837, XT −372.024 253. [c] Reference 12. [d] Despite an extensive search, full convergence of the displacements was not obtained; frequency calculations were not performed on this geometry. However, the forces were well within the convergence criteria. [e] This structure was optimized with the C_1–C_6 bond held at 2.728 Å. [f] Energy above the complexed NC activation energy. [g] The sum of the Mulliken charges on the butadiene fragment, in units of electrons. [h] The relative Coulombic potential energy based on the Mulliken charges.

Background. Diels–Alder reactions are, in general, concerted, with both bonds partially formed at the transition state.[4] The experimental support for this mechanism includes (1) the retention of stereochemistry in the reactions of disubstituted reagents, as in eq 2,[6] (2) the secondary deuterium kinetic isotope effects on the forming bonds, eq 3,[7] and (3) quantitative measures of cooperativity in disubstituted dienophiles as examined by either optical induction[8] or activation energies (eq 4.)[9] In only a few cases is there evidence for zwitterionic intermediates in Lewis acid catalyzed reactions, and these are between reagents especially able to stabilize the zwitterion, as in eq 5.[10] Although semiempirical calculations[5d,11] suggest a two-step or two-stage reaction, RHF[12,13] and MCSCF[14] ab initio calculations provide theoretical support for the concerted (and in the case of butadiene and ethylene, synchronous) mechanism.

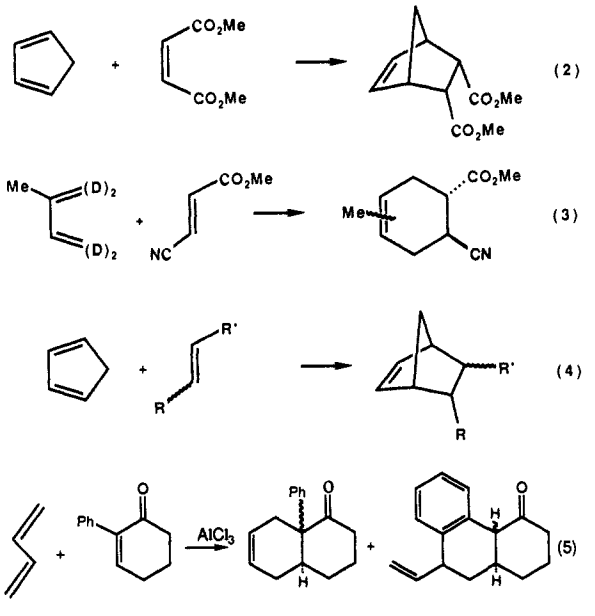

Table II. Activation Energies for the Thermal and Lewis Acid Catalyzed Cycloadditions of Butadiene and Acrolein

	ΔE(act)			vibrational[d] correction
	STO-3G[a]	3-21G[b]	6-31G*[c]	
catalyzed				
NC	26.2	21.6	34.9	
XC	28.1	23.8	36.4	1.70
NT	28.0	26.3	36.8	1.94
XT	29.5	28.9	39.1	1.64
uncatalyzed				
NCU	35.5	30.5	41.9	
XCU	35.9			
NTU	35.6	32.6	42.5	
XTU	36.2			

[a] RHF/STO-3G. [b] RHF/3-21G. [c] RHF/6-31G*//RHF/3-21G. [d] On the basis of the sum of the zero-point energy and thermal energies. This number is to be added to the activation energy.

Since Diels and Alder first recognized the stereospecificity and endo selectivity of the diene cycloaddition, there have been many explanations for the selectivity of the Diels–Alder reaction. Frontier molecular orbital theory (FMO) and in particular the Woodward–Hoffmann rules[5a] provided a theoretical framework in which to understand the concerted nature of the reaction. Houk[15] and others[5c,16] have explained the regiochemical preferences of substituted dienes and dienophiles in terms of the maximum overlap of the largest coefficients of the HOMO and LUMO. Hehre[17] has recently suggested that the electrostatic potentials of the reactants can explain the regioselectivities of disubstituted reagents. Endo selectivity was first rationalized by Alder[18] as due to the "maximum accumulation of unsaturation". Woodward and Hoffmann,[5a] and subsequently Houk,[15] Salem,[19] and Alston,[16a] have explained endo selectivity in terms of secondary orbital interactions. Others have suggested dipole–dipole,[20] charge transfer,[21] electrostatic,[17] and steric interactions[4] as important. Houk[5b] has further suggested that the effect of Lewis acid catalysts is to lower the dienophile LUMO energy, bringing it closer to the diene HOMO. This allows for a stronger interaction and lowers the activation energy. Complexation also polarizes the dienophile LUMO, increasing the coefficients at both the β and carbonyl carbons, which then increases the regioselectivity and the endo

(6) See ref 4, especially footnote 108.
(7) Gajewski, J. J.; Peterson, K. B.; Kagel, J. R. *J. Am. Chem. Soc.* **1987**, *109*, 5545–5546.
(8) Tolbert, L. A.; Ali, B. *J. Am. Chem. Soc.* **1984**, *106*, 3806–3810.
(9) Hancock, R. A.; Wood, B. F., Jr. *J. Chem. Soc., Chem. Commun.* **1988**, 351–353.
(10) Thompson, H. W.; Melillo, D. G. *J. Am. Chem. Soc.* **1970**, *92*, 3218–3220.
(11) Dewar, M. J. S.; Pierini, A. B. *J. Am. Chem. Soc.* **1984**, *106*, 203–208.
(12) Loncharich, R. J.; Brown, F. K.; Houk, K. N. *J. Org. Chem.* **1989**, *54*, 1129–1134.
(13) (a) Houk, K. N.; Lin, Y.-T.; Brown, F. K. *J. Am. Chem. Soc.* **1986**, *108*, 554–556. (b) Bach, R. D.; McDouall, J. J. W.; Schlegel, H. B. *J. Org. Chem.* **1989**, *54*, 2931–2935.
(14) Bernardi, F.; Bottini, A.; Field, M. J.; Guest, M. F.; Hillier, I. H.; Robb, M. A; Venturini, A. *J. Am. Chem. Soc.* **1988**, *110*, 3050–3055.
(15) Houk, K. N. *Tetrahedron Lett.* **1970**, 2621–2624.
(16) (a) Alston, P. V.; Ottenbrite, R. M.; Cohen, T. *J. Org. Chem.* **1978**, *43*, 1864–1867. (b) Ahn, N. T.; Seyden-Penne, J. *Tetrahedron* **1973**, *29*, 3259–3265.
(17) Kahn, S. D.; Pau, C. F.; Overman, L. E.; Hehre, W. J. *J. Am. Chem. Soc.* **1986**, *108*, 7381–7396.
(18) Alder, K. *Annalen* **1951**, *571*, 87.
(19) Salem, L. *J. Am. Chem. Soc.* **1968**, *90*, 553–566.
(20) Berson, J. A.; Hamlet, Z.; Mueller, W. A. *J. Am. Chem. Soc.* **1962**, *84*, 297–304.
(21) Woodward, R. B.; Baer, H. *J. Am. Chem. Soc.* **1944**, *66*, 645.

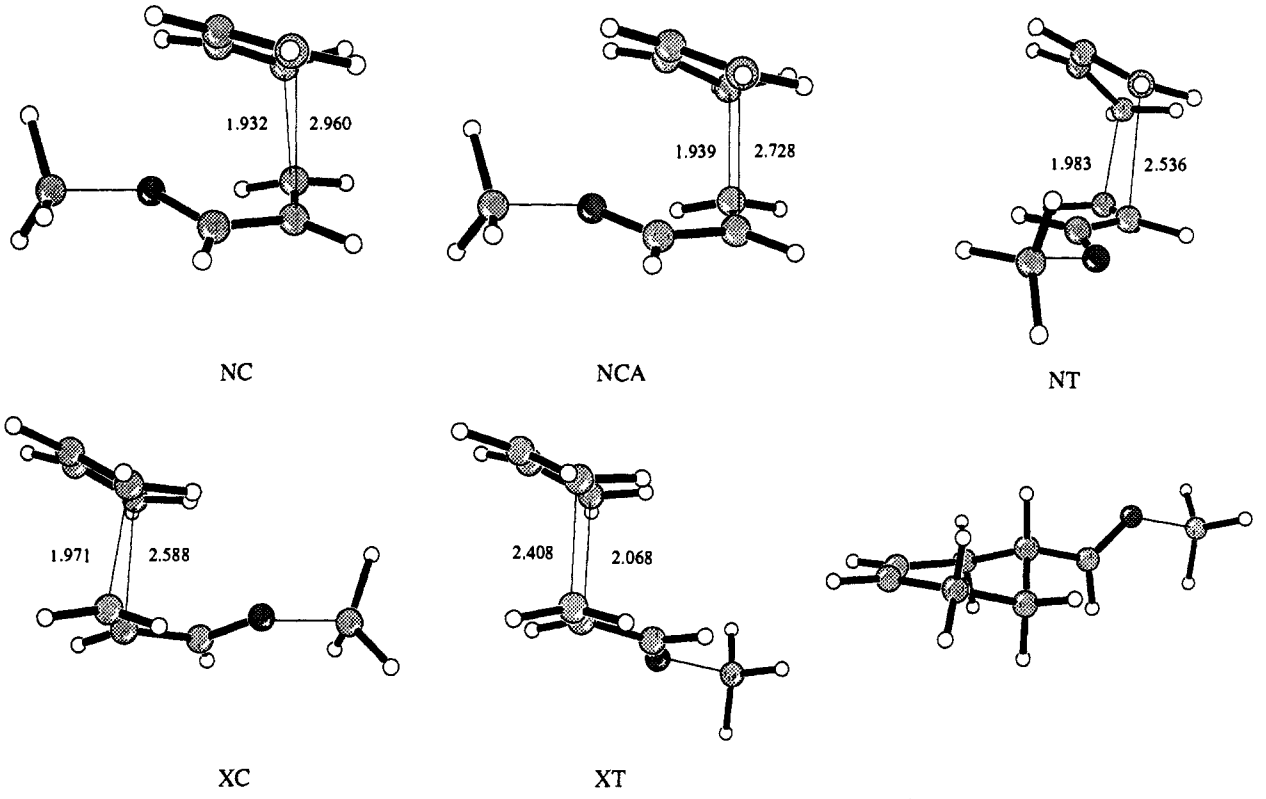

Figure 1. The 3-21G transition structures and coordinated product. Forming bond lengths are given in Å.

preference, respectively. Houk[5b] has also suggested that the transition state for the catalyzed reaction is earlier and tighter than the uncatalyzed, leading to higher diastereoselectivity. On the basis of semiempirical calculations, Branchadella, Oliva, and Bertran[5d] have suggested that BF_3 catalysis changes the reaction of cyclopentadiene and acrolein from a one-step to a two-step mechanism.

Calculational Details. Four transition structures were located with RHF ab initio molecular orbital theory, using the GAUSSIAN 86 program,[22] first with the STO-3G basis set[23] and then with the 3-21G basis set.[24] Single-point calculations were carried out with the 6-31G* basis set[25] on the RHF/3-21G geometries. Unless otherwise specified, the structures discussed below are those optimized at the RHF/3-21G level (Table I), and the energies are those calculated at the RHF/6-31G* level (Table II). The relative energies are not affected by the zero-point energies and thermal corrections. These are given in Table II. The endo *s-trans* and *s-cis* transition structures (NT and NC) were also optimized at the RHF/6-31G* level. This made only small changes in the bond lengths and angles. (See the supplementary material for details.) The four transition structures (NC, NT, XC, XT) and the related point NCA, along with the product, are shown in Figure 1.

Acrolein can add either endo (N) or exo (X), in either an *s-cis* (C) or *s-trans* (T) conformation. Lewis acids complex to carbonyls in the molecular plane, either syn or anti to the olefin. Experimentally[26] and theoretically,[27] the syn complexes of acrolein and boranes are less stable than the anti ones; consequently, transition structures were located only for the four anti complexes, sketched below. Frequency calculations for all the structures were performed at the RHF/STO-3G level, and also at the RHF/3-21G level for NT, XC, and XT. These all showed one imaginary frequency corresponding to the formation of the two new σ bonds. NC is the most stable transition structure, while XT is the least stable of the four located; these two represent extremes in most other properties as well (Table I). An additional structure, NCA, is described below. In contrast to the semiempirical calculations, these are all transition structures, not intermediates.

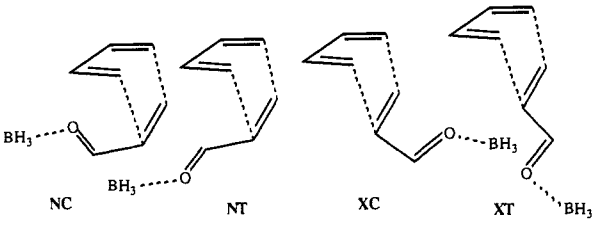

The flexibility of the endo *s-cis* transition structure made locating the transition structure quite difficult. NC was found by holding the C_1–C_6 distance fixed and optimizing the remainder of the structure, then adjusting the distance and reoptimizing. NCA was another structure encountered during the course of this exploration of the potential energy surface, described below.

Energetics. While RHF theory has been shown to reproduce qualitatively the transition state of the parent Diels–Alder reaction,[13,14] the question remains as to whether it is adequate to describe the bonding changes in the catalyzed reaction. The activation energy for the catalyzed reaction is calculated to be 34.9 kcal/mol (21.6 kcal/mol at the RHF/3-21G level). This is substantially above the experimental value of 10.4 ± 1.9 kcal/mol for the $AlCl_3$ catalyzed addition of methyl acrylate to butadiene.[28] The RHF/6-31G* and RHF/3-21G levels also overestimate the activation energy for the uncatalyzed reaction. The calculated values are 41.9 and 30.5 kcal/mol, respectively,[12]

(22) GAUSSIAN 86, release C: Frisch, M.; Binkley, J. S.; Schlegel, H. B.; Raghavachari, K.; Martin, R.; Stewart, J. J. P.; Bobrowicz, F.; DeFrees, D.; Seeger, R.; Whiteside, R.; Fox, D.; Fluder, E.; Pople, J. A., Carnegie Mellon University, Pittsburgh, PA.

(23) Hehre, W. J.; Stewart, R. F.; Pople, J. A. *J. Chem. Phys.* **1969**, *51*, 2657.

(24) Binkley, J. S.; Pople, J. A. *J. Am. Chem. Soc.* **1970**, *102*, 939.

(25) Hariharan, P. C.; Pople, J. A. *Theor. Chim. Acta* **1973**, *20*, 213.

(26) Torri, J.; Azzaro, M. *Bull. Soc. Chim. Fr.* **1978**, II-283-291.

(27) (a) Loncharich, R. J.; Schwartz, T. R.; Houk, K. N. *J. Am. Chem. Soc.* **1987**, *109*, 14–23. (b) Guner, O. F.; Ottenbrite, R. M.; Shillady, D. D.; Alson, P. V. *J. Org. Chem.* **1987**, *52*, 391–394. (c) LePage, T. J.; Wiberg, K. B. *J. Am. Chem. Soc.* **1988**, *110*, 6642–6650. (d) Birney, D. M.; Houk, K. N. Unpublished results.

(28) Inukai, T.; Kojima, T. *J. Org. Chem.* **1967**, *32*, 872–875.

as compared to an experimental value of 19.7 kcal/mol.[29] The same trend is found for the reaction of butadiene and ethylene (45.0[13b] and 38.3[13a] kcal/mol, respectively, as compared to 26–35 kcal/mol experimentally[13]) and for many other allowed pericyclic reactions.[30] This is due to the limitation of the single-configuration RHF wave function as discussed elsewhere.[30] In those calculations of allowed pericyclic reactions carried out with the inclusion of electron correlation, single-point energies on RHF geometries gave activation energies in much closer agreement with experiment.[30] On the other hand, geometry optimizations including correlation make only small changes in the geometries. This lends additional credence to the RHF geometries reported here.

A better test of the reliability of calculations at the RHF level is to examine the trends in the activation energies presented in Table II. The calculated activation energy of the catalyzed reaction (NC) is 7.0 kcal/mol lower (9 kcal/mol by RHF/3-21G) than that of the uncatalyzed one (NCU.) This compares well with the similar reaction of butadiene and methyl acrylate for which $AlCl_3$ catalysis lowers the activation energy by 9.3 kcal/mol.[28] The calculated endo selectivity (ΔE for two transition structures) increases from 0.3 kcal/mol to 1.5 kcal/mol (*s-cis*) or from 1.3 kcal/mol to 2.3 kcal/mol (*s-trans*) upon Lewis acid complexation. This may be compared with the reaction of methyl acrylate and *trans*-1,3-pentadiene, for which the 0.2 kcal/mol endo preference in the uncatalyzed case increases to 1.8 kcal/mol upon $AlCl_3$ catalysis.[31] The question of whether the *s-cis* or the *s-trans* conformation of acrolein is present in the transition state is not answered by experiment. The products from Diels–Alder reactions of chiral acrylate esters suggest that they proceed through an *s-trans* conformation,[2a,32] while reactions of chiral vinyl ketones and acrylamides appear to give products resulting from an *s-cis* conformation.[2c,33] In our calculations for the catalyzed reaction, the *s-cis* structures are more stable than *s-trans* by 1.9 and 2.7 kcal/mol for endo and exo pairs, respectively. Less *s-cis* selectivity was found in the thermal case, amounting to only 0.6 kcal/mol for endo and 1.7 kcal/mol for exo (6-31G*//STO-3G).[12]

Heat of Reaction. The complex of 4-formylcyclohexene and BH_3 was optimized at the RHF/3-21G level. This gives an overall heat of reaction of −39.8 kcal/mol for the addition of *s-trans*-butadiene and *s-trans*-acrolein·BH_3. For the uncatalyzed reaction, the heat of reaction is −39.9 kcal/mol. The exothermicity of the reaction is unchanged by the catalyst, and the lower activation energy of the catalyzed reaction must be due to other factors, as discussed below.

Geometry

Asynchronicity. Recently, there has been significant controversy as to whether the parent Diels–Alder reaction is synchronous or not, although experiments[7-9] and recent MCSCF[14] calculations fully support the synchronous mechanism. With as asymmetric a dienophile as acrolein complexed by a Lewis acid, one would not expect a synchronous reaction. Experimental studies by Tolbert and Ali,[8] and by Gajewski[7] concur with this general expectation, and our calculations reflect it quite dramatically, as seen in the front views in Figure 2. While the transition structure for the parent reaction of ethylene and butadiene has forming bond lengths of 2.210 Å each, the structure for the uncatalyzed reaction of butadiene and acrolein (NCU) has bond lengths of 2.088 and 2.353 Å and that for the catalyzed reaction (NC) has bond lengths of 1.932 and 2.96 Å. There is only slightly greater asynchronicity in NT at the RHF/6-31G* level as compared to RHF/3-21G, with the C_1–C_6 distance 0.08 Å longer and the C_4–C_5 distance 0.05 Å shorter. The asynchronicity of the catalyzed reaction is also manifest in the pyramidalization of the reacting centers. Carbons 4 and 5 of NC are both pyramidalized[34] by 11°, while carbons 1 and 6 on the longer forming bond are nearly planar (2° and 3°, respectively). The lowest energy structure, NC, has the most pronounced asynchronicity, while XT has the highest energy and is more synchronous. The asynchronicity makes the steric requirements quite different at either of the forming bonds.

The asynchronicity is readily understood in terms of frontier molecular orbital theory. The large coefficient on the β carbon of the acrolein LUMO causes this terminus to be much more electrophilic than the carbon α to the carbonyl, which has a very small coefficient. Greater overlap at β with the diene HOMO leads to a stronger and shorter bond at the transition state. Despite the dramatic asynchronicity in the catalyzed transition structures, especially NC, the calculations indicate that the reaction is still concerted, since no energy minimum corresponding to an intermediate has been found. Bond formation at the β carbon is far more advanced that at the α carbon, but there is nonetheless some bond formation there as well. This is evidenced by the normal mode displacements of the calculated imaginary frequencies at each of the transition structures in the catalyzed reaction; Figure 3 shows carbons 1 and 6 of NC moving together. It is also manifest in the Mulliken population analysis, which shows positive overlap of 0.018 between carbons 1 and 6 in NC and 0.037 in NT. While this is much smaller than the values of 0.079 and 0.067 between carbons 4 and 5 in NC and NT, it does indicate some bonding between carbons 1 and 6.

Flexibility. The weakness of the bonding to the α carbon leads to considerable flexibility in the transition structure. Whereas in the parent reaction all four atoms involved in the formation of the new σ bonds are coplanar, in the catalyzed reaction there can be substantial twisting about the stronger forming bond (C_4–C_5.) The dihedral angle C_1–C_4–C_5–C_6 is sensitive to steric, electrostatic, and bonding interactions, and it varies dramatically from 5° in NC to −18° in NT, as seen in the top views of Figure 2. The normal modes associated with the harmonic frequencies provide a further indication of the flexibility of the transition structures. In NT, for example, the torsion around the C_4–C_5 bond is calculated to have a frequency of only 76 cm^{-1} (unscaled). For comparison, the smallest real vibration (71 cm^{-1}) corresponds to bending the BH_3 out of the plane of the acrolein, and the third vibration (121 cm^{-1}) is the rotation around the B–O bond. The harmonic approximation is especially unsuited for these weak modes, but this does illustrate the flexibility of the structures. As a separate indication of this flexibility, comparison of the structures NC and NCA shows that large geometrical changes are possible with only minor changes in the energy (vide infra.)

Charge Separation. As two molecular fragments approach each other, they experience destabilizing interactions between filled orbitals, and these interactions may be understood as the origin of the activation barrier to orbital symmetry allowed reactions.[35] In the "normal" electron-demand Diels–Alder reaction, there is stabilizing interaction involving charge donation from the diene HOMO to the dienophile LUMO. However, there is also an interaction between the diene LUMO and dienophile HOMO, and thus only small net charge donation. In the case of the Lewis acid catalyzed reaction, the low activation energy has been explained by a narrowing of the diene HOMO–dienophile LUMO gap resulting in more charge donation.[5b] This is observed in the catalyzed transition structures calculated here, as given in Table I. In the uncatalyzed structure NCU, there is only 0.09 electron transferred from butadiene to acrolein, but in the catalyzed structure NC there is net transfer of 0.31 electrons, according to the Mulliken population analysis. This is quite remarkable for a gas-phase reaction and will become even larger in solution. The Mulliken charge distribution[36] and the geometry reflect the

(29) Kistiakowski, G. B.; Lacher, J. R. *J. Am. Chem. Soc.* **1936**, *58*, 123–133.
(30) (a) Spellmeyer, D. C.; Houk, K. N. *J. Am. Chem. Soc.* **1988**, *110*, 3412–3416. (b) Jensen, F.; Houk, K. N. *J. Am. Chem. Soc.* **1987**, *109*, 3139–3140.
(31) Inukai, T.; Kojima, T. *J. Org. Chem.* **1967**, *32*, 869–871.
(32) Curran, D. P.; Kim, B. H.; Piyasena, H. P.; Loncharich, R. J.; Houk, K. N. *J. Org. Chem.* **1987**, *52*, 2137–2141.
(33) Evans, D. A.; Chapman, K. T.; Bisaha, J. *J. Am. Chem. Soc.* **1988**, *110*, 1238–1256.
(34) Haddon, R. C. *Acc. Chem. Res.* **1988**, *21*, 243–249.
(35) Houk, K. N.; Gandour, R. W.; Strozier, R. W.; Rondan, N. G.; Paquette, L. A. *J. Am. Chem. Soc.* **1979**, *101*, 6797–6802.

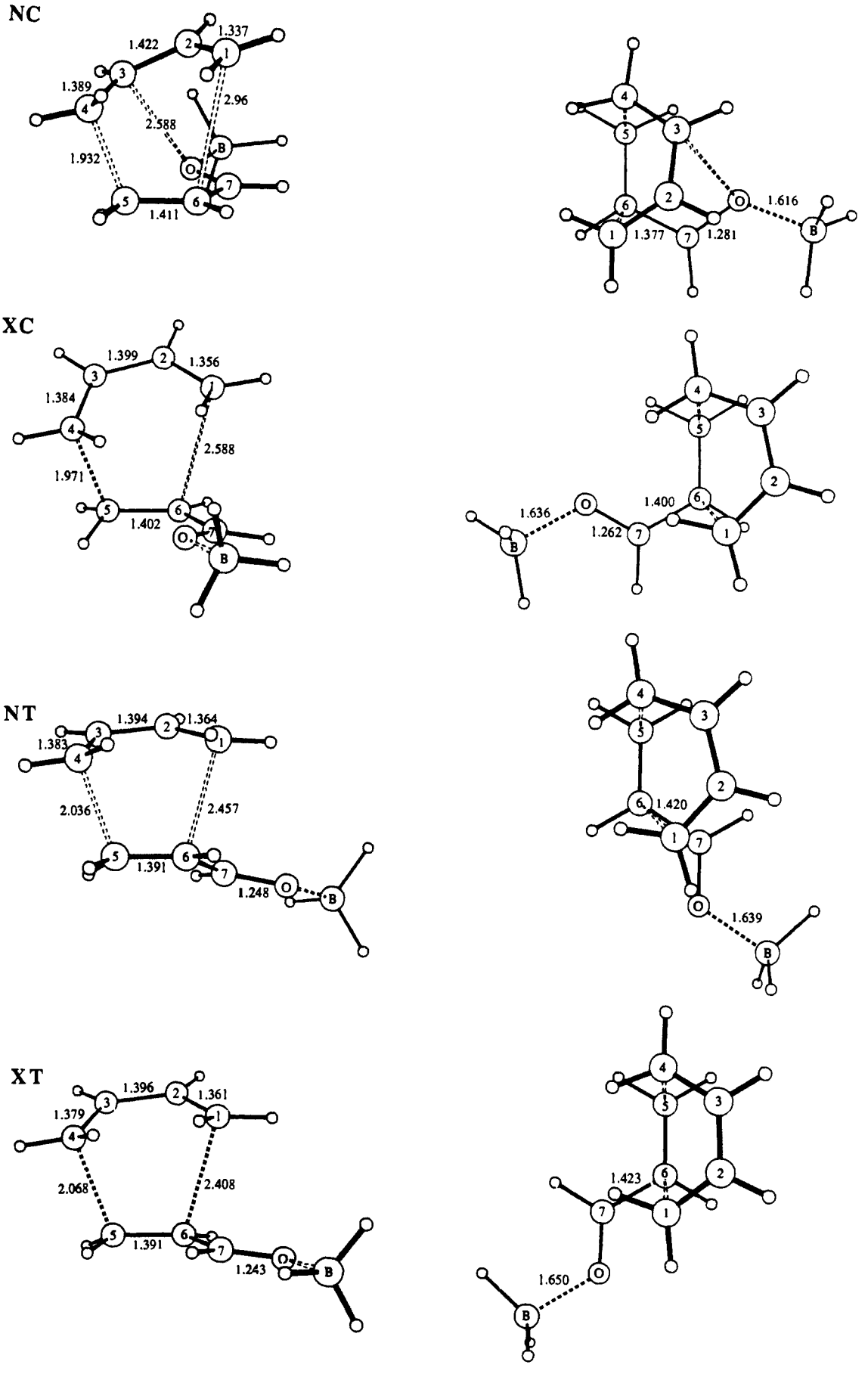

Figure 2. Front and top views of the *endo-s-cis* (NC), *exo-s-cis* (XC), *endo-s-trans* (NT), and *exo-s-trans* (XT) transition structures at the RHF/3-21G level for the cycloaddition of butadiene to acrolein complexed with BH_3. Distances are in Å.

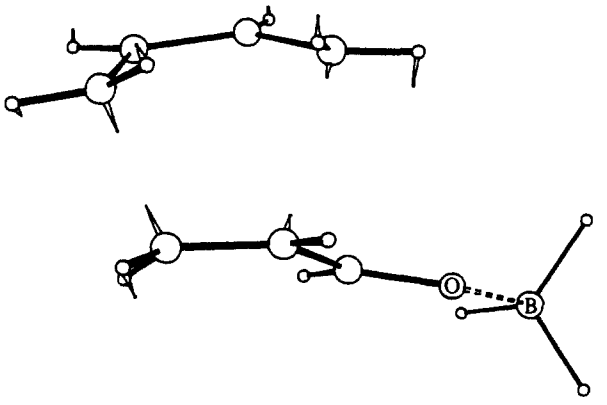

Figure 3. RHF/3-21G transition vector for structure NT.

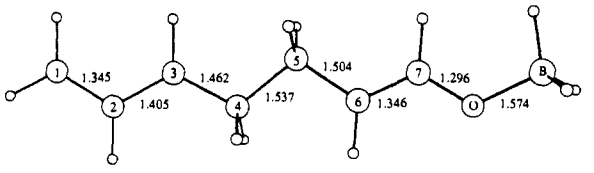

Figure 4. Extended zwitterion with C_s symmetry, at the RHF/3-21G level.

zwitterionic character of the transition structure. The positive charge in the butadiene fragment is centered on carbons 1 and 3, as in an allyl cation, and the negative charge is on the BH_3, the oxygen, and carbon 6, as in an enolate anion. The enolate character leads to lengthening of the C_7–O bond in the NC transition structure (1.281 Å) as compared to either the complexed starting material (1.228 Å) or the product (1.225 Å) and likewise a shortening of the O–B distance (1.616 Å vs 1.691 and 1.696 Å, respectively.) The allyl cation character in NT is manifested by the bond lengths of C_1–C_2 (1.361 Å) and C_2–C_3 (1.396 Å), which are similar to those in the 1-methylallyl cation (1.357 and 1.387 Å, respectively, RHF/3-21G). The ability of a substituted diene to stabilize this positive charge will be important in determining regiochemistry.

Although the HOMO–LUMO interactions are stabilizing, the resulting charge separation is necessarily destabilizing. We have crudely estimated the degree of electrostatic interaction between the two fragments by summing the Coulomb attraction between Mulliken charges centered on the atomic centers. The relative energies calculated in this way are shown in Table I. It is initially surprising that the structure with the greatest charge separation (NC) has the lowest Coulomb energy. Because of its coiled geometry, the charges, although larger in magnitude, are closer together in space, and hence the Coloumb energy is lower overall. Overall this simple electrostatic model reproduces, but exaggerates, the energetic trends in the ab initio calculations. The stability of the *exo-s-trans* structure in particular is underestimated by this method.

The dipole moment calculation is independent of the Mulliken population analysis and hence provides an alternative view of the degree of charge separation. The dipole moment of *s-trans*-butadiene is zero by symmetry, while that of *s-cis*-acrolein complexed with BH_3 is 7.1 D and that of the *s-trans* complex is 7.8 D. The calculated dipole moment of 8.4 D in NC is lower than those of the other transition structures, which range up to 10.0 D for NT, again reflecting the coiled geometry of NC. Overall the dipole moments are not substantially larger than those of the reactants. In both the reactants and the transition structures, the dipole moment is less for the *s-cis* conformation, but in ground-state acrolein the difference is insufficient to change the preferred conformation.

(36) We are aware of the limitations of Mulliken charge analysis, (see, for example: Grier, D. L.; Streitweiser, A., Jr. *J. Am. Chem. Soc.* **1982**, *104*, 3556) but the trends reported here are likely to give qualitative indications of charge and bonding.

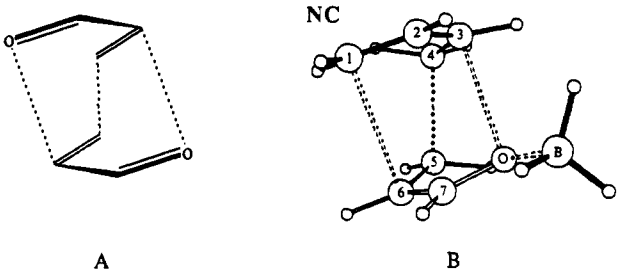

Figure 5. (A) Symmetrical transition state for the dimerization of acrolein. (B) A view of NC from the same perspective.

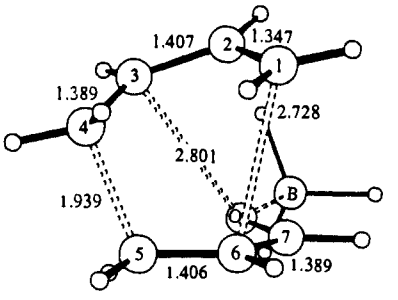

Figure 6. Structure of NCA at the RHF/3-21G level.

The extreme case of charge donation corresponds to the formation of a zwitterionic intermediate. A fully extended zwitterion (C_s symmetry, Figure 4) was optimized at the RHF/3-21G level. This extremely unstable structure had an energy 48.8 kcal/mol above that of the lowest energy transition structure. Not unexpectedly, this structure is not a minimum; when the constraint of C_s symmetry was lifted, this structure optimized toward the cyclized product. Such an unsolvated zwitterion is not an adequate model for the solution-phase reaction, in which solvation would provide considerable stabilization. Nonetheless, the extremely large dipole moment of this extended zwitterion (29.6 D) makes is incompatible with the modest solvent effects observed experimentally.[37]

A coherent picture of the endo selectivity now emerges, in which the stabilizing diene HOMO–dienophile LUMO interaction leads to a destabilizing substantial charge donation. Because the geometry of NC minimizes the physical separation of the induced charges, greater charge transfer is permitted in this case. Consequently, this transition structure has the lowest energy.

Secondary Orbital Interactions. Woodward and Hoffmann suggested that the origin of endo selectivity in the Diels–Alder reaction was "secondary orbital interactions",[5a] that is, interactions not leading to bonds in the product. They discussed the dimerization of butadiene, in an *endo-s-trans* geometry, but an extension to this system suggests that there should be a bonding interaction between C_2 and C_7 in the NC and NT structures. The signs of the HOMO and LUMO coefficients are appropriate for positive overlap, and the orbital coefficient on C_7 is quite large in the ground state. In view of these factors, most other authors have also focussed on this particular secondary orbital interaction. However, in the structures calculated here, there is little evidence for this interaction; the Mulliken overlap population between C_2 and C_7 is negative, −0.011 for NC and −0.006 for NT. There is positive overlap between C_3 and O in NC, however, with a value of 0.031. This interaction was considered by Salem in a discussion of the transition state for the dimerization of acrolein.[19] In this case it is possible to imagine a symmetrical structure (as in Figure 5A) in which the primary and secondary interactions would be of equal magnitude at the transition state. In such a case, there would necessarily be a bifurcation beyond the transition state,

(37) Yamamoto, H.; Maruoka, K.; Furuta, K.; Ikeda, N.; Mori, A. In *Stereochemistry of Organic and Bioorganic Transformations*; Bartmann, W., Sharpless, K. B., Eds.; VCH Publishers: New York, 1987; pp 13–21.

where the reaction partitioned to two distinct, but symmetry equivalent, products.[38]

This latter secondary orbital interaction is extremely important in NC (see Figure 5B). The overlap population between C_1 and C_6 is only 0.018, which is substantially smaller than the so-called "secondary" overlap between C_3 and O. Indeed these latter two atoms are closer together (2.588 Å) than C_1 and C_6 (2.960 Å) between which a bond is formed experimentally. The structure NC might lead to the formation of vinyldihydropyran. However, the potential surface is extremely flat. Structure NCA (Figure 6) lies on the potential ridge separating reactants from products. It has a shorter C_1–C_6 distance (2.728 Å) and a longer C_3–O distance (2.820 Å) than NC, but it is only 0.05 kcal/mol higher in energy at the 3-21G level. Indeed, RHF/6-31G* single-point calculations place NCA 0.2 kcal/mol below NC. Except for the slight twisting of the plane of the butadiene relative to the acrolein which leads to the difference in bond lengths, there are no further major differences between NC and NCA. Indeed we found a number of similar structures on the potential ridge separating reactants and products, all of which had similar energies, and similar Coulombic attractions.

There is much greater diastereoselectivity in the catalyzed Diels–Alder reactions of chiral acrylates as compared to the uncatalyzed reactions. The facial selectivity is presumably due to steric effects from the chiral auxiliary. One would expect that these would be mitigated by both the longer C_1–C_6 bond distance and the softer torsional potential. However, the energies of the competing transition structures must also be considered. For the uncatalyzed case,[12] NC and NT are only 0.6 kcal/mol apart, and the reaction will proceed to some extent through both pathways. For chiral reactants, and assuming steric factors give 100% diastereoselectivity in each transition structure, this still gives two diastereomers as determined by the relative barrier heights. In contrast, for the catalyzed case, NT is 1.5 kcal/mol higher than NC, resulting in greater selectivity. Additionally, the strong Coulombic interactions may favor closer approach of some atoms not directly involved in bond formation, which would then permit a greater steric differentiation of diastereomeric transition structures than in the uncatalyzed case.

(38) Stanton, R. E.; McIver, J. W., Jr. *J. Am. Chem. Soc.* **1975**, *97*, 3632–3646. See Figure 2.

Conclusion

The concerted, but very asynchronous, catalyzed Diels–Alder reaction proceeds via a transition structure with one strong and one weak forming bond. The latter imparts considerable flexibility to the structures. FMO interactions as well as the resulting charge separation and dipolar interactions are important factors in the reaction. Together these factors lead to the lowering of the activation energy and to the enhancement of the endo selectivity and regioselectivity commonly observed upon catalysis.

Acknowledgment. We are grateful to the National Science Foundation for financial support of this research and for generous grants of computer time at the Pittsburgh Supercomputing Center. Jeffrey D. Evanseck provided valuable assistance on computations and graphics.

Registry No. BH_3, 13283-31-3; butadiene, 106-99-0; acrolein, 107-02-8.

Supplementary Material Available: Full geometries and energies of all the transition structures (12 pages). Ordering information is given on any current masthead page.

Calculations of p*K* Differences between Structurally Similar Compounds

Alexander A. Rashin,*,† James R. Rabinowitz,‡ and Jason R. Banfelder†

Contribution from the Department of Physiology and Biophysics, Mount Sinai School of Medicine of the City University of New York, New York, New York 10029, and Environmental Protection Agency, Research Triangle Park, North Carolina 27711. *Received May 18, 1989*

Abstract: An attempt is made to find out whether accurate calculations of p*K* differences in a series of biologically active compounds are feasible. The computational method used employs a combination of quantum mechanical calculations of the vacuum proton affinities and a new method for calculation of hydration energies based on a continuum representation of the solvent. We demonstrate that our method leads to good agreement with experimental results and results of the free energy perturbation method in calculations of tautomeric equilibria and some computational "mutation" simulations. Application of our method to the calculations of p*K* differences between congeners of imidazolium shows that experimental values of such differences can be computationally predicted within one p*K* unit for pairs of congeners differing in the hydrogen to methyl substitution or in the position of the same substituent in the molecule. However, calculated values deviate from the experimental ones by more than four p*K* units for the pairs of congeners differing in the substitution of the hydrogen or methyl group to the chloro or nitro group. The deviations from experimental values found for these substitutions may be attributed to errors in the calculated proton affinities in vacuum that do not cancel for substitutions involving groups with very different chemical properties. These findings suggest a practical restriction on the quantitative calculations of p*K* differences to narrow classes of compounds. Computations of p*K* differences performed for three congeners of the neurotransmitter histamine from such a class lead to the results that agree with experimental physiological data.

Many chemical and biochemical phenomena in solution are governed by relatively small free energy differences. Such phenomena include conformational and tautomeric equilibria, proton transfer between two groups, differential ligand binding, p*K* differences between closely related compounds, etc. The commonality and importance of these phenomena made them a popular object of experimental and theoretical studies.[1-7] Until

† Mount Sinai School of Medicine.
‡ Environmental Protection Agency.

(1) Aue, D. H.; Webb, H. M.; Bowers, M. T. *J. Am. Chem. Soc.* **1976**, *98*, 318.
(2) Pullman, A.; Pullman, B. *Quart. Rev. Biophys.* **1975**, *7*, 505.

0002-7863/90/1512-4133$02.50/0